APPLIED PHYSICS

Досліджено можливість оцінки рівня зносу стволів артилерійських гармат за акустичними полями пострілів. Незважаючи на важливість знання поточного стану стволу, існуючі методи оцінки зносу недостатньо оперативні. Ці методи дають досить наближені оцінки або вимагають дорогого устаткування. На відміну від відомих методів, пропонований в статті метод оперативний, не вимагає великих витрат, може бути поєднаний з тренувальними стрільбами та легко автоматизується. Досліджено характеристики балістичної і дульної хвиль, що утворюються при пострілі з гармати, показані відмінності їх параметрів для стволів без зносу і стволів з критичним рівнем зношеності. Критеріальним показником зносу служить початкова швидкість снаряда. Показано, що за акустичними характеристиками постріл зі ствола, що має будь-яку ступень зносу, еквівалентний пострілу з гармати меншого калібру. Проведено обчислювальний експеримент на реальних акустичних сигналах, що зареєстровані при стрільбі 155 мм гаубиці. Обрано інформативні ознаки акустичних сигналів від пострілів, що дозволяють автоматично класифікувати стволи на два класи – стволи, придатні до використання, і стволи зі зносом, що перевищує критичний. Показано, що застосування методу опорних векторів (SVM) дозволяє впевнено класифікувати стволи за рівнем зносу на підставі часових і спектральних ознак балістичної і дульної хвиль. При аналізі акустичних сигналів від пострілів застосований кумулятивний аналіз спектральних характеристик. Це дало можливість суттєво підвищити ймовірність правильної класифікації стволів. Отримані результати корисні для практичного застосування в артилерійських підрозділах в польових умовах. Результати досліджень дозволяють розробити автоматизовану систему оцінки стану стволів з високою оперативністю, що забезпечує достатню в бойовій практиці точність оцінки рівня зносу стволів

Ключові слова: знос артилерійського ствола, початкова швидкість снаряда, балістична хвиля, дульна хвиля

UDC 62-503.57
DOI: 10.15587/1729-4061.2020.206114

DEVELOPMENT OF A METHOD FOR DETERMINING THE WEAR OF ARTILLERY BARRELS BY ACOUSTIC FIELDS OF SHOTS

E. Dobrynin
Researcher
National University "Odessa Maritime Academy"
Didrichsona str., 8, Odessa, Ukraine, 65029
E-mail: 20artuxa62@gmail.com
M. Maksymov
Doctor of Technical Sciences,
Professor, Head of Department
Department of Computer Automation Technologies*
E-mail: prof.maksimov@gmail.com
V. Boltenkov
PhD, Associate Professor
Department of Information Systems
Institute of Computer Systems*
E-mail: vaboltenkov@gmail.com
*Odessa National Polytechnic University
Shevchenka ave., 1, Odessa, Ukraine, 65044

Received date 12.05.2020
Accepted date 23.06.2020
Published date 30.06.2020

1. Introduction

The barrel is one of the main units in present-day artillery systems. It is a part of an artillery gun designed to direct a shell during shooting and impart the required velocity to it [1].

The barrel condition largely determines the combat qualities of the gun in general. Barrel wear refers to all irreversible changes in the surface of the barrel channel caused by the impact of shots on it. The barrel wear is not only a change in the size and shape of its channel but also a change in the roughness of its surface, the formation of a network of surface cracks, chemical, and structural transformations in its material. Wear is usually divided into erosion wear arising from thermomechanical effects of powder gases; mechanical wear caused by mechanical effects of leading elements of the shell on the channel surface and chemical wear brought about by chemical interaction of powder gases and the barrel metal [2]. Wear of the barrel channel entails the worsening of combat qualities of the gun and the effectiveness of its use [3]. Ultimately, wear can be considered as an integral process leading to the final result: a decrease in initial shell velocity and an increase in its spread from shot to shot as a random variable [4].

In addition to the military-applied aspect, the artillery barrel wear has a material economic aspect. The cost of barrels of current large-caliber artillery systems is estimated at 30–35 % of the cost of the system in general. Further operation of the barrel which has reached the maximum level of wear can lead to its complete, irrecoverable failure. In this case, the measures of replacement and disposal of out-of-service barrels lead to large economic and time losses.

The methods used today for assessing wear of artillery barrels are either obsolete and rather approximate or based on modern technologies requiring expensive job-dedicated equipment. The latter methods are very costly and time-consuming. At the same time, it is known that an artillery shot creates powerful acoustic fields that can be recorded at sufficiently large distances. According to [5], analysis of the acoustic fields accompanying firing can be used to find out

the type of guns, shell caliber, and other data characterizing the artillery system. Unfortunately, such prospects are presented in [5] at a level of general considerations. According to the preliminary estimates, methods of acoustic analysis are simple, economical, requiring no expensive equipment and applicable in the field. Therefore, study of the possibility of assessing wear of the artillery gun barrels by the acoustic fields generated by shots is a fairly relevant scientific and applied problem.

2. Literature review and problem statement

Known methods for assessing barrel wear can be divided into two classes: firing methods, that is, those requiring firing from the diagnosed barrel and firing-free methods. The simplest and oldest method of a rough wear estimation implies firing at vertical shields installed at a distance of 40–60 m in which oval holes are broken [1]. The hole ovality is estimated as a ratio of the size of the long axis l_{long} to the size of the short axis $l_{short} - K_{oval} = l_{long} / l_{short}$. If the value K_{oval} exceeds 1.5 for at least one hole, the barrel is rejected. The method is empirical, theoretically insufficiently substantiated and the obtained estimates of wear are very approximate. More modern methods for assessing the barrel wear are based on ascertaining the barrel condition by accurate measurement of the muzzle shell velocity by means of specialized radar devices. In Russian and Ukrainian sources, these devices are called ballistic radar stations (BRS) or artillery ballistic stations (ABS) [6]. In English literature, the name muzzle velocity radar (MVR) is used [7].

The BRSs are centimeter range Doppler radars mounted on a tripod in the immediate vicinity of the muzzle section or on the gun cradle [8]. These methods provide the high accuracy of prompt measurement of the initial velocity. However, they have a series of shortcomings. The high cost of an equipment set is the main shortcoming. In addition, a substantial amount and weight of equipment, low noise immunity, in particular, low stealth and resistance to mutual interference when working in battle formations [9] are also the BRS drawbacks. Advanced designs of the BRS operating in the millimeter-wave range [10] are free from the latter drawbacks but the high cost is the main obstacle to their mass introduction in artillery units. Firing-free barrel diagnostic methods are divided into the calculation and instrumental methods. Calculation methods are based on calculating residual barrel life according to statistical models and the history of combat use of the gun (the shots number, charge, ammunition) [11, 12]. These methods are rather laborious [13] and the reliability of their results in relation to a concrete gun has not been confirmed [14]. Instrumental methods imply the inspection of the inner barrel surface to assess wear [15]. The oldest method of inside barrel examination implies a mechanical examination. When examining barrels in this way, control discs or other calibrated gauges attached to a rod are inserted into the barrel bore from the breech. When using mechanical measuring tools for assessing wear, the subjective aspect, that is the operator qualification is of great importance. Besides, such methods of instrumental wear control are characterized by high complexity and insufficient accuracy [16]. Endoscopes are the next generation of instrumental methods of wear control [17]. They enable a fairly detailed study of the condition of the inner barrel surface, presentation of its image in any projection [18], and quantitative processing of the measurement data [19]. Endoscopic methods of barrel control were brought to a robotic level [20]. These methods make it possible to get complete and accurate information about the degree of barrel wear, however, they have a disadvantage of high equipment cost and laboriousness. The integration of instrumental methods of various types is presented in [21] in the form of an artillery control and check machine. However, such a solution is costly that makes it inapplicable in the troops.

Characteristics of acoustic signals arising from shots were analyzed in [22–24]. For example, characteristics of shock waves from artillery shots are studied in [22]. Article [23] addresses the recognition of howitzer caliber from acoustic signals of the shot. The results of finding out the location of the artillery firing position by the acoustic method are presented in [24, 25]. Although the studies [22–25] do not directly address the issue of assessing the barrel wear, they create prerequisites for the studies in this direction.

Analysis of data published in [1–25] makes it possible to establish the following. Existing methods for assessing the degree of wear of artillery barrels are diverse. However, the methods available for widespread use in the military are ideologically outdated, provide low accuracy of assessment, and practically are unsuitable for automation. The methods based on modern technologies require expensive equipment which is an obstacle to their practical implementation in military units. At the same time, there are prerequisites for applying a prompt, inexpensive, and easily automated method of analyzing the acoustic signals accompanying artillery shots to solve the problem of the barrel wear assessment. However, this issue has not been sufficiently studied both in theoretical and practical terms. Such a study has become the subject of this paper.

3. The aim and objectives of the study

The study objective concerns development of a method for identifying the condition of artillery barrels based on an analysis of acoustic signals accompanying shots to determine maximum allowable wear levels.

To achieve this objective, it was necessary to solve the following tasks:

– to develop a simulation model of acoustic signals of artillery shots from barrels with various wear levels based on experimental data and form sets of synthesized records for various barrels;

– to extract informative attributes of signals for automatic assessment of barrels by the degree of their wear;

– to develop a method of binary classification of artillery barrel wear level based on the extraction of informative attributes of acoustic signals during automatic classification;

– to conduct a computational experiment with the classification of the level of barrel wear and assess qualitative indicators of classification.

4. A simulation model of acoustic signals when firing from worn barrels

A gunshot is accompanied by the formation of two types of acoustic waves: a shock wave (SW) and a muzzle wave (MW) [26]. When a shell moves along a certain trajectory, the shock wave with a conical front (Mach cone) is

generated. Its center moves with the moving shell. The cone opening angle is

$$\theta_M = \arcsin 1/M, M>1, 0<\theta_M<\pi/2, \quad (1)$$

where M is the Mach number equal to $M=V/s$; V is the initial velocity of the shell and s is the velocity of sound in air at current meteorological parameters.

The acoustic signal of the SW has a characteristic N-shape with rising and falling fronts of about 1 μs duration at the beginning and end of the signal. The SW signal is broadband, its total duration for artillery shots is 3–8 ms. The bandwidth of the SW signal is from 1 kHz to 10 kHz. The shock waveform is determined by the Wightman model [27], which describes its parameters as follows:

$$A = \frac{0.53P_0\left(M^2-1\right)^{1/8}\phi}{d_{sM}^{3/4}l^{3/4}}[\text{Pa}], \quad (2)$$

$$T_N = \frac{1.82Mld^{1/4}\phi}{c\left(M^2-1\right)^{3/8}l^{1/4}} \approx \frac{1.82\phi}{c}\left(\frac{Md}{l}\right)^{1/4}, \quad (3)$$

where

$$t_r = \frac{\lambda}{c}\frac{P_0}{A}$$

is the duration of the rise (fall) front; A is the SW amplitude; T_N is the duration of the main section of the pulse; P_0 is the atmospheric pressure; ϕ is the shell caliber; l is the shell length; d_{sM} is the shortest distance from the recording point to the Mach cone; $t_r \approx t_d$ is the duration of the SW pulse rise and fall fronts, respectively; λ is the mean free path of an air molecule ($\lambda \approx 6.8\times10^{-8}$ m for air under normal conditions).

Fig. 1 shows a typical SW signal (*a*) and its energy spectrum calculated by the method of Welch periodograms (*b*) [28].

Attributes of the SW:

– the SW is observed and recorded by a microphone installed on the ground surface only if the observation point lies inside the Mach cone;

– the velocity of the shell during its flight decreases and, at some trajectory point, it may become less than the velocity of sound and the SW will disappear, so it must be recorded at small distances from the firing point;

– due to the short front of the SW rise, it must be recorded with a high sampling rate.

The muzzle wave (MW) is created by the expansion of high-pressure gases after the shell leaves the barrel. The acoustic signal of the MW propagates with the velocity of sound c from the muzzle section of the gun barrel into the environment. The sound pressure level of the MW is about 150 dB near the barrel muzzle section. The MW is a pulse signal with a duration of 30–50 ms having a frequency spectrum in the range from 8–10 Hz to 100 Hz [29]. The MW signal is also broadband, however, its frequency bandwidth in the spectral region is an order of magnitude smaller than that of the SW. The MW form is described by the Friedlander-Reed model [30]:

$$P_{mw} = A_{mw}\left(1-\frac{t}{T_0}\right)e^{-\beta t/T_0}, \quad (4)$$

where A_{mw} is the pulse amplitude; T_0, β are the pulse form parameters.

Due to the frequency-dependent sound attenuation in air, the MW form quickly turns into a damped vibrational pulse [31]. Experiments with the MW records of real artillery shots have shown that this waveform is well approximated by the Berlage model widely used in seismology at distances greater than 50 m from the barrel muzzle section [32]:

$$P_{mw}^B = A_{mw}t^{nr}e^{-\alpha t}\sin\left(f_o t\right), \quad (5)$$

where nr is the indicator of the rate of rising of the front edge of the MW; α is the indicator of attenuation rate of the oscillatory process of the MW; f_o is the dominant frequency.

Fig. 2 shows the MW signal described by the Friedlander-Reed model with the following parameters: A_{mw}=300 Pa, T_0=50 ms, β=28 (line 1). The same signal calculated with taking into account atmospheric attenuation [33] at a distance of 10 m from the muzzle section is shown by line 2. The same signal approximated by the Berlage model with parameters A_{mw}=300 Pa, nr=5, α=0.52, f_o=20 Hz is depicted by line 3. It can be seen that the Berlage model quite accurately describes the MW form.

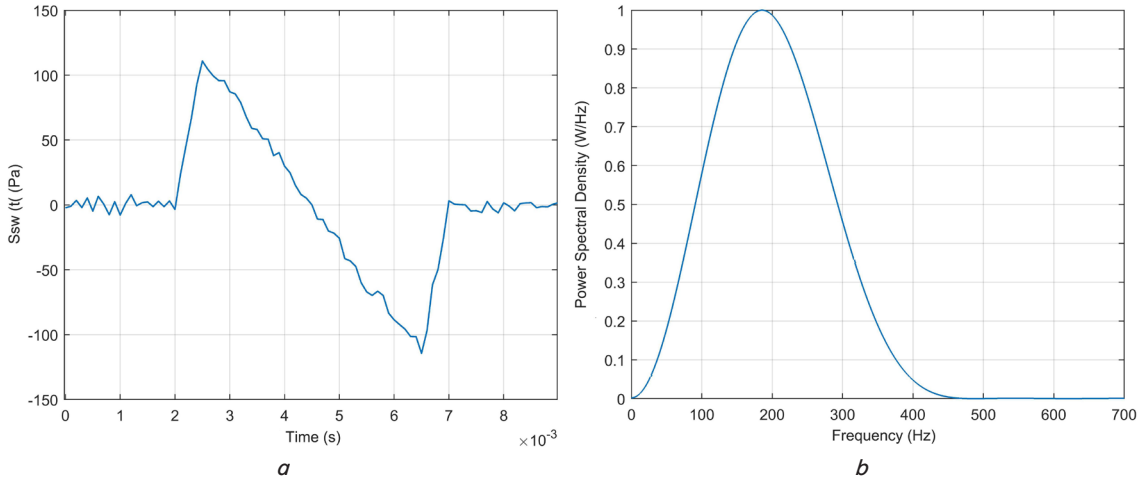

Fig. 1. Signal of the shock wave: *a* – temporal pattern; *b* – energy spectrum

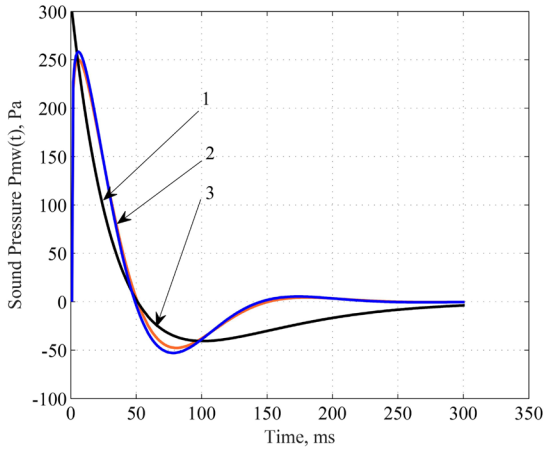

Fig. 2. The MW signal: 1 — as described by the Friedlander-Reed model; 2 — the signal calculated with taking into account atmospheric attenuation; 3 — the signal approximated by the Berlage model

Further, the Berlage model (5) will be used to describe the MW. Its attributes are as follows. In contrast to the Friedlander model (4), it is described by a continuous function which makes it more convenient for mathematical operations. In addition, it was shown that the pulse-shaped signal described by the Berlage model is the minimum phase signal [32]. For such signals, their main energy is concentrated in the initial section of the pulse. Therefore, when analyzing the minimum phase signals, it is sufficient to analyze the first period of the oscillatory process. Fig. 3 shows a typical form of the SW pulse-shaped signal (*a*) and its energy spectrum (*b*).

Attributes of the MW: the MW propagates from the point of its formation with the velocity of sound *c*. The MW front is spherical, however, with a sufficient degree of approximation, it can be considered flat at distances greater than 50 m from the muzzle section. It has been practically established that for distances less than 2–3 km, the MW amplitude is 2–3 times higher than the SW amplitude [26].

Let us consider some definitions from the theory of artillery firing [34]. Muzzle energy $E_m = qV^2/2$ is the kinetic energy of the translational motion of a shell having mass q at the moment of it leaving the barrel bore with velocity V. When assessing a gun, the magnitude of the muzzle energy is considered as a comparative characteristic of the gun might. (When calculating, the rotational motion of the shell is not taken into account). The coefficient of the gun might $C_E = E_m/\phi^3$ expresses the ratio of the muzzle energy to the cube of the gun caliber ϕ. The coefficient of the gun might shows how much energy falls on a conventional unit of the barrel channel volume when firing from a given gun.

Introduce the concept of barrel wear coefficient:

$$\eta = V^*/V, \quad 0 < \eta < 1, \tag{6}$$

where V^* is the initial velocity of the shell when fired from the worn barrel. The maximum permissible minimum η is 0.9 for ground artillery in armies of post-Soviet countries [12], and 0.85 in the armies of NATO and China [3]. Then, the gun might for the worn barrel is

$$C_E^* = q\left(V^*\right)^2/2\left(\phi^*\right)^3, \tag{7}$$

that is, a shot from a gun with a wear coefficient η, ceteris paribus (gun type, charge, firing conditions) is equivalent to a shot from a gun of reduced caliber ϕ^*. To fulfill the condition $C_E^* = C_E$ (muzzle energy is determined by the energy of the given type of charge), we can introduce the concept of conditional equivalent caliber (CEC) ϕ^*, which, proceeding from (7), is equal to

$$\phi^* = \phi\eta^{2/3}. \tag{8}$$

Obviously, $\phi^* < \phi$, since η<1. It was indicated above that according to the experimental data, the SW and MW parameters depend on the gun caliber, that is, the smaller caliber the shorter pulse of the SW and duration of its first half-period. Thus, the last expression provides prerequisites for modeling the barrel wear according to parameters of the SW and MW accompanying the shot.

Next, it is necessary to experimentally verify the possibility of classification of barrels by the level of their wear based on the assumptions made. To this end, at the next step of the study, it is necessary to form a set of records of acoustic signals corresponding to shots from standard and worn barrels.

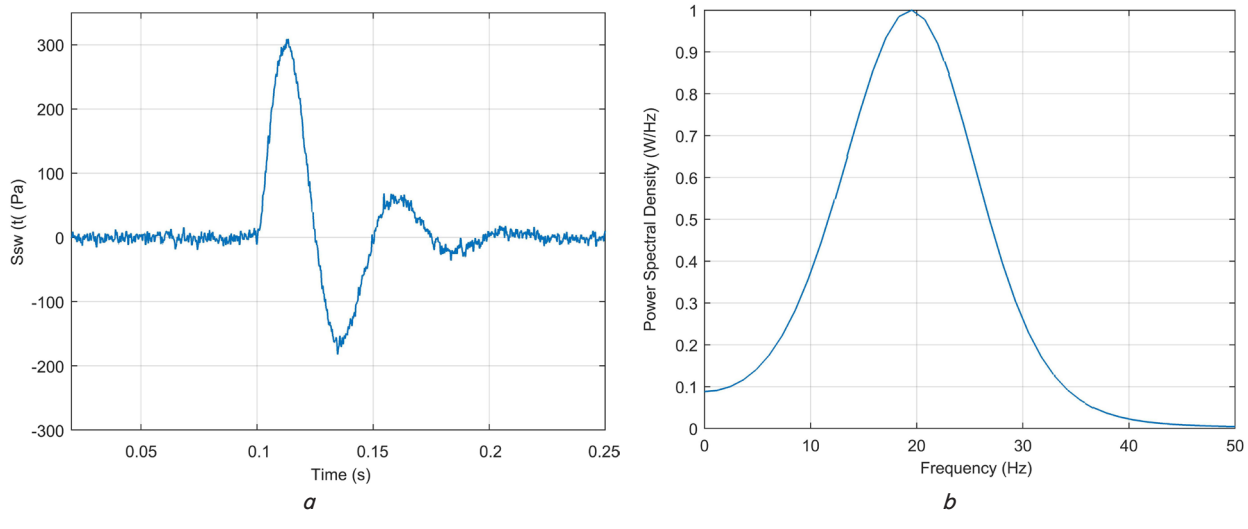

a *b*

Fig. 3. Signal of the muzzle wave: *a* — temporal pattern; *b* — energy spectrum

5. Formation of sets of the synthesized records of acoustic signals for various barrels

To ascertain the possibility of assessing the barrel wear by the acoustic signals from shots, a computational experiment was carried out. The general diagram of its stages is shown in Fig. 4.

Based on the considered Wightman and Berlage models for the MW, CEC for the MW and actual signals, a set of synthesized records was formed. At the next stage of the study, informative attributes are extracted for constructing an automatic classifier for defect-free and worn barrels. Next, a classifier is built, trained, and tested on a test sample of classification results and their quality.

Actual records of acoustic signals made during the M109A3GN howitzer [35] firing were taken as the study basis. The howitzer barrel (NATO designation: 1025–25–136–2638) was 6045 mm (39 calibers) long. The M107 shell was used, the maximum charge was 5 DM72 modules, initial velocity (tabular) was 684 m/s. Signals were recorded by broadband measuring microphones at distances of 20 m and 250 m from the firing position. Besides, the characteristics of howitzer shots given in [36] and actual records of the shock wave signals from howitzer shots [37] were used.

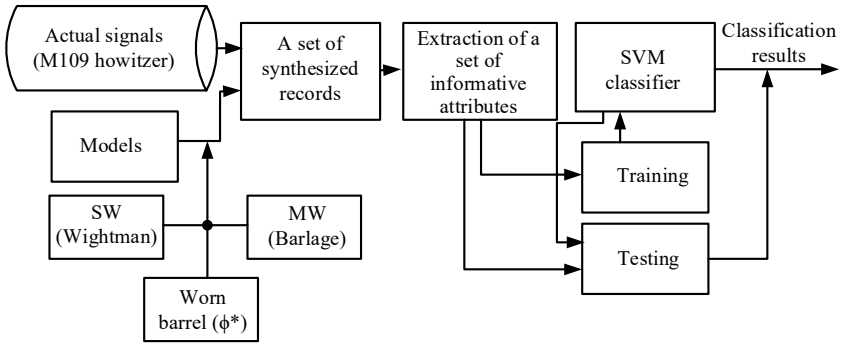

Fig. 4. Diagram of a computational experiment for studying the assessment of barrel wear by acoustic signals from shots

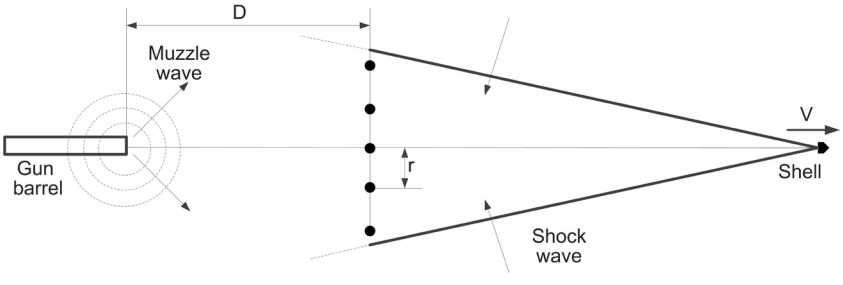

Fig. 5. Geometric diagram of the simulated situation

Based on the digitized records of signals, a set of 300 records was formed. The records simulated acoustic signals from artillery shots in real conditions.

The procedure for forming a record set. Fig. 5 shows a general geometric diagram of a simulated real firing situation (plan view where lateral shell drift was not taken into account).

Microphones in a quantity of N=5 that recorded the SW and MW from the shots were installed on the ground at a distance of D=250 m from the barrel muzzle section along a line perpendicular to the projection of the firing trajectory at a distance of r=20 m from each other. The microphone recording start was synchronized with the shot. After the shot, each microphone recorded acoustic signals for 0.6 s. The use of several microphones is explained by the following:

1) since random normally distributed noise implementations and random recording parameters are specified for each of the microphones, the use of N microphones enables an N-time increase in the data set volume;

2) the reliability of finding and estimation of the SW and MW parameters against the noise background increases; this is especially important in real field conditions.

The distance D=250 m was taken from the following considerations. Assessment of the degree of barrel wear by a drop of initial shell velocity should be made close enough to the firing position while the shell velocity is close to the initial velocity. In addition, the phenomenon of refraction of sound rays can be observed during the propagation of acoustic waves in the surface layer of the atmosphere. It is caused by the presence of vertical temperature and the wind velocity gradients that can greatly distort parameters of acoustic signals.

According to [38], the neutral nature of sound propagation is always observed at a distance of less than 500 m from the wave source and the refraction effect on acoustic signals is excluded for sure. The distance r=20 m between microphones was taken from the following considerations. On the one hand, they can have different observation conditions concerning the signal-to-noise ratio (SNR). On the other hand, all microphones used for SW recording must be within the Mach cone created by the flying shell. With a microphone line size of 80 m, the last condition is satisfied at any initial shell velocities.

For each of the simulated shots, an acoustic signal was synthesized on a microphone with a sampling frequency of 10 kHz.

Taking into account the additive nature of noise, the synthesized record was constructed according to the following model:

$$s(t)=s_{sw}(t)+s_{mw}(t)+s_{noise}(t), \quad (9)$$

where $s_{sw}(t)$ is the signal fragment including the SW pulse; $s_{mw}(t)$ is the signal fragment including the MW pulse; $s_{noise}(t)$ is the realization of a 0.6 s long noise signal.

The procedure of synthesis of a record simulating a shot from an unworn barrel is as follows. Since the SW always arrives at the microphone earlier than the MW (as $V<c$), the SW signal is placed at the beginning of the record as a 5 ms fragment cut from a real record. Next, there is a 200 s "blank section" corresponding to the time delay of the SW and MW arrival to the microphone. Then, a 0.395 ms fragment with the MW record is placed at the end of the "blank section". The general diagram of the formation of the synthesized record is shown in Fig. 6.

For the most complete simulation of a real situation when forming a record fragment with the MW, a phenomenon of the MW reverberation was taken into account, that is, the reflection of the MW from the earth's surface which lengthens the real MW signal [39]. The reverber-

ation was modeled by pinning two MW reflections to its pulse "tail":

$$s_{mw\_reverb}(t) = s_{mb0}(t) + s_{mv\_refl1}(t) + s_{mb\_refl2}(t), \quad (10)$$

where $s_{mw\_reverb}(t)$ is the MW signal taking into account the reverberation; $s_{mb0}(t)$ is direct MW signal;

$$s_{mv\_refli}(t) = s_{mb0}(t - \tau_i) \cdot K_{refl}{}^{i}, \ (i = 1,2),$$

K_{refl} is the coefficient of the MW reflection from the earth's surface taken equal to 0.6 according to [39]; τ_i is the time delay of arrival of the i-th MW reflection taken from the relation $\tau_i \in rand$ [5, 20] ms; *rand* is the standard operator of generating a pseudo-random number within the range of [0; 1].

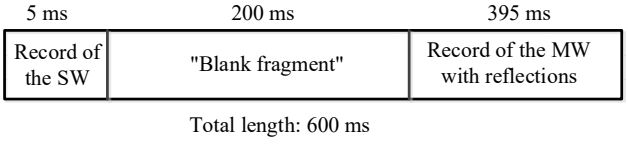

Fig. 6. Diagram of synthesized record formation

Let us consider separately modeling the noise accompanying record of the SW and MW signals during their propagation in the bottom layer of the atmosphere. The signals of acoustic waves are of low-frequency during firing. Analysis of real signal records from [35] has shown that the noise generated by the standard operators of the generation of pseudorandom numbers *rand* and *randn* poorly simulates the noise component actually observed in the records since they form a spectrum of uniform frequency. In fact, the noise of wind around the microphones is the main real acoustic noise in the low-frequency region (below 500 Hz) [40]. As shown in [41], wind noise is a special random process in the stationarity interval with a spectral density falling with a frequency f as $1/f$. This is the so-called "pink noise". The noise interference spectrum is shown in Fig. 7, *a*.

In this regard, pink noise was specially generated for modeling the wind noise with the use of the Teager–Kaiser filtering algorithm given in [42]. The resulting spectrum of the generated noise is shown in Fig. 7, *b*. Analysis of real shot records has shown that the model of wind noise as a pink noise is in a good agreement with the noise realizations observed in the experimental records.

Formation of records simulating a shot from a worn barrel is harder. In accordance with [2], the maximum permissible value of the coefficient of barrel wear η=0.9 was chosen for the experiment. To synthesize a concrete record, the value of $\eta_i = rand$[0.9; 0.95] was chosen where $i \in [1, NRF]$; NRF is the total number of records simulating a worn barrel. For the obtained value of η_i, the conditional equivalent caliber ϕ_i^*. for a given shot was calculated from relation (8). At the SW modeling stage, the SW parameters were calculated for the obtained value of CEC ϕ_i^* from relations (2) and (3) and the SW signal was constructed with a sampling step of 0.0001 s. After constructing the SW signal, its parameters (amplitude, duration of the rise and fall fronts, and total duration) were compared with the corresponding experimental tabular values from [37]. If the deviations did not exceed 20 %, then the SW signal was included in the synthesized record. Otherwise, a new value of η_i was generated and the step of SW formation was repeated. In the formation of the synthesized MW signal based on the ϕ_i^* calculated for a given i, an empirical expression [36] relating the caliber and the dominant frequency f was used:

$$f_0^*[\text{Hz}] = 1{,}850 / \phi[\text{mm}]. \quad (11)$$

For the given ϕ_i^*, f_0^* was calculated from the last expression. Next, the MW signal selected from real records was approximated by the Berlage model (5) in which f_o was replaced by f_0^*. The MW signal which was embedded in the record was calculated by the Berlage model modified in this way.

After the formation of all records, wind noise in the form of the additive pink noise described above was superimposed on these records. The SNR was calculated as:

$$SNR = \frac{\sum_{j=1}^{N0} s^2(j)}{\sigma_{pink}^2}, \quad (12)$$

where $s(j)$ are counts of the generated record (nonzero only in the intervals of the presence of SW and MW); $N0$ is the length of the window corresponding to the duration of the SW and MW in the counts; σ_{pink} is the dispersion of the pink noise.

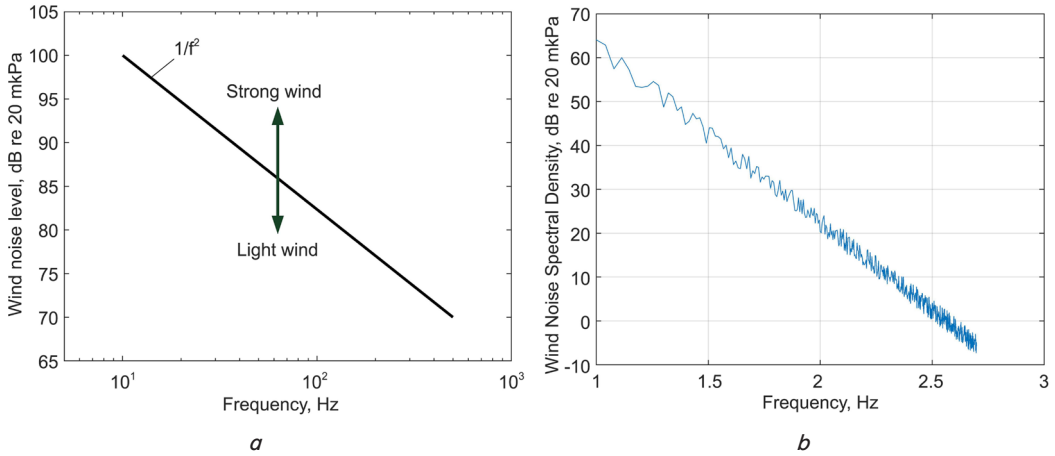

a *b*

Fig. 7. Spectral density of the wind noise: *a* — theoretical, according to [41]; *b* — obtained in modeling by pink noise

Taking into account the additive nature of the wind noise, each synthesized record was constructed according to the following model:

$$s(t)=s_{sw}(t)+s_{mw}(t)+s_{noise}(t),$$

where $s_{sw}(t)$ is the signal fragment including the SW pulse; $s_{mw}(t)$ is the signal fragment including the MW pulse; $s_{noise}(t)$ is the implementation of a noise signal with a length equal to the record length.

According to the described procedure, two arrays of digital data were formed constituting a set of signal records including two classes. Class 1 contained records of acoustic signals of the shots from barrels with a coefficient of wear $s_{noise}(t)$. This class will be called SB (serviceable barrel). Class 2 contained records of signals with a coefficient of barrel wear above critical value: $\eta^* \approx 0{,}9$, that is the WB class (a worn barrel). The data set consisting of 150 records in each class was broken into training and test samples.

Taking into account the additive nature of the wind noise, each synthesized record was constructed according to the following model:

$$s(t)=s_{sw}(t)+s_{mw}(t)+s_{noise}(t),$$

where $s_{sw}(t)$ is the signal fragment including the SW pulse; $s_{mw}(t)$ is the signal fragment including the MW pulse; $s_{noise}(t)$ is the implementation of a noise signal with a length equal to the record length.

Fig. 8 shows a typical synthesized record for SNR=10 dB (a defect-free barrel, η=0.98). The arrows in Fig. 8 show the areas of the SW and MW reflection. Red marks indicate the time of arrival of the SW and MW. Section SW of the same record is shown in Fig. 1, *a* in an enlarged time scale.

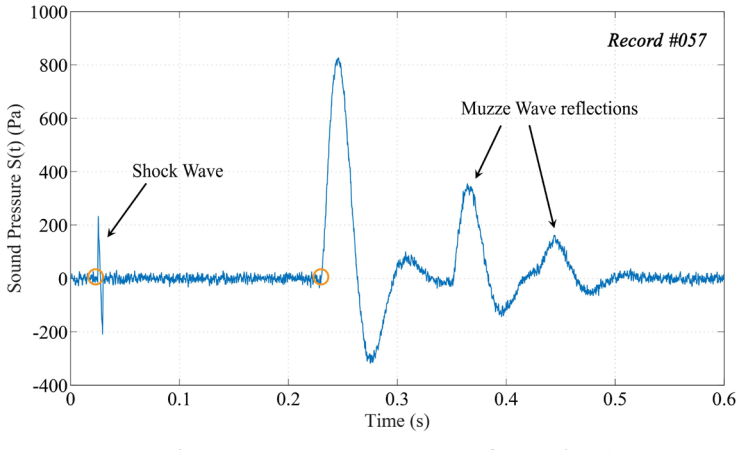

Fig. 8. Typical synthesized record (SNR=10 dB)

At the next study stage, informative attributes were extracted and a method for automatic binary classification of barrels by the level of their wear was developed.

6. Extraction of informative attributes of signals. Development of a method of binary classification for determining wear of artillery barrels

All automatic classifiers require sets of informative attributes that must be extracted from synthesized sets of records. To proceed with the construction of an automatic barrel classifier according to the level of wear, the records were pre-processed to form informative attributes. To extract informative attributes of the signals, it is important to identify the moment of the SW and MW arrival in the record as accurately as possible. Since the SW and MW signals are random broadband signals, the Kailats-Price-Urkovits energy detector was used to detect and assess the moment of the SW and MW arrival [43]. Such a detector is described in sufficient detail in [44]. It has shown good results in extracting acoustic signals on the noise background. The moments of the SW and MW arrival extracted by such a detector are shown in Fig. 8 by red marks.

For automatic classification of barrels according to a set of informative attributes, the method of support vectors, or a support vector machine (SVM), was chosen [45]. The SVM is the algorithm of learning with a teacher. The algorithm is ideally suited for the task of diagnosing barrels since it was originally created to break the statistical samples into two classes. The main idea of the SVM method is as follows. Each object to be classified is represented by a point (or a vector describing the point coordinates) in an n-dimensional space. A point can belong to one of two classes. As a result of applying the SVM, a hyperplane of dimension $(n-1)$ that separates the classes is constructed. As a result of applying the method, an optimal separating hyperplane is formed in such a way as to ensure maximum margin between the classes which guarantees the best quality of classification. Parameters of the SVM classifier are chosen in the training set. Next, the classifier parameters are checked on the test data sample. The method is described in sufficient detail in [46]. The SVM method has been successfully used to classify acoustic images [47] including artillery sound signals.

Let us proceed to the construction of the attribute space for classification. This space is used in the training and test samples. After identification of sections containing the SW and MW signals, a set of informative attributes is formed in each record. The informative attributes can be divided as follows:

1. The shock wave: attributes in the time domain (Fig. 9, *a*).

1. 1. The SW amplitude, A_{SW}.

1. 2. The rate of growth of the SW front edge, $\mathrm{d}/\mathrm{d}t\,T_{rise}$.

1. 3. The moment of the first intersection of the first zero by the SW signal, T_{SW0}.

2. Shock wave: attributes in the spectral region (it can be seen from Fig. 9, *c* that general patterns of the SW and MW spectrum are similar. Patterns of the spectra are schematically represented in Fig. 9 by one illustration although the frequency scale of the SW and MW spectra differs by an order of magnitude).

2. 1. The central frequency of the SW spectrum, f_0.

2. 2. The width of the SW spectrum by level is 3 dB from the maximum Δf value.

Cumulant apparatus (CA), a progressive tool for studying spectra of pulsed random processes [48], turned out to be an extremely useful instrument for analysis of the SW and MW signals in the spectral domain. The CA is based on the calculation of cumulants (central moments of the 3rd and 4th orders), kurtosis of the signal spectrum, that is, "sharpness of the peak" of the spectral power density. For a discrete signal

$x(n)$, an N-point discrete Fourier transform $X(m)$ is calculated. The kurtosis (the central moment of the 4th order) is calculated as in [49]:

$$KS = \frac{M}{M-1}\left[\frac{(M+1)\sum_{i=1}^{M}\left|X_i(m)^4\right|}{\left(\sum_{i=1}^{M}\left|X_i(m)\right|^2\right)^2} - 2\right]. \quad (13)$$

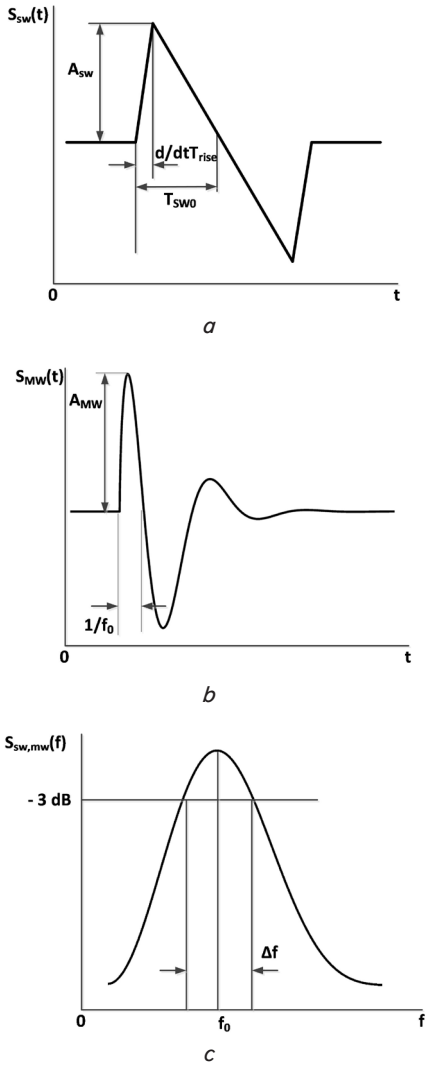

Fig. 9. Informative attributes of signals: *a* — the shock wave, time domain; *b* — the muzzle wave, time domain; *c* — the shock wave and the muzzle wave, spectral domain

In terms of the kurtosis content, there is a measure of the difference between the shape of the signal spectrum and the Gaussian curve. Further development of the CA was a kurtogram [49] which is a graphic image of successive kurtosis values calculated over the pulse duration in a sliding window. To illustrate the information content of the CA, Fig. 10 shows the SW kurtograms of shots from the unworn barrel: η=1 (*a*) and the worn barrel for η=0.87 identified from the synthesized records. The kurtogram was calculated using the standard function of the MATLAB kurtogram system.

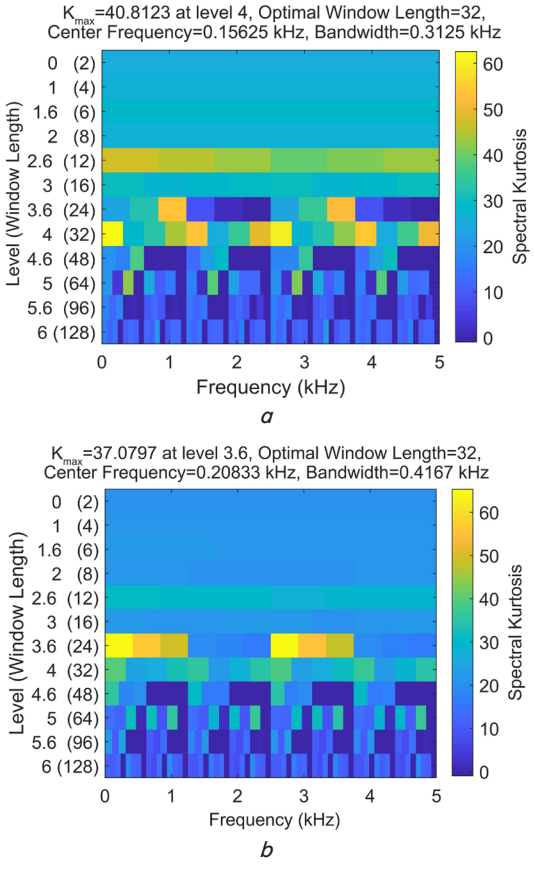

Fig. 10. Kurtograms of the SW from shots: *a* — firing from an unworn barrel; *b* — firing from a worn barrel

It should be noted that the kurtogram function also calculates the center frequency and the spectrum bandwidth already selected above as informative attributes of signals in the spectral domain. Since the kurtogram as a graphic image cannot be used directly for the SVM classifier, then based on the CA, integral cumulant attributes were included in the number of informative attributes in a separate subset of the frequency domain:

3. Shock wave: cumulant attributes in the spectral domain.

3. 1. Kurtosis of the SW spectrum, KS.

3. 2. The skewness of the SW spectrum [50], the central moment of the third order:

$$SkewS = C\sum_{i=1}^{M}\left(X_i - \bar{X}\right)^3, \quad (14)$$

where

$$C = \frac{m(m+1)}{(m-1)(m-2)(m-3)\sigma_X^4},$$

$\bar{X}$ and σ_X are the mathematical expectation and standard X, respectively.

SkewS can be either positive (skewness of the spectrum to the left relative to the vertical axis of the Gaussian curve) or negative (skewness to the right).

4. Muzzle wave: attributes in the time domain (Fig. 9, *b*).

4. 1. The SW amplitude, A_{MW}.

4. 2. Duration of the first half-cycle of the oscillatory process, $1/2f_0$, for the MW, this is f_0, the dominant frequency.

4. 3. Assessment of nr parameter of the Berlage model obtained by approximating the SW signal.

4. 4. Estimation of the α parameter of the Berlage model obtained by approximating the SW signal.

5. Muzzle wave: attributes in the spectral domain (Fig. 9, *c*).

5. 1. Central (dominant) frequency of the MW spectrum, f_0.

5. 2. Width of the MW spectrum by the level: 3 dB from the maximum Δf value.

6. Muzzle wave: cumulant attributes in the spectral domain.

6. 1. Kurtosis of the MW spectrum, *KS*.

6. 2. Spectrum skewness, *SkewS*.

Thus, 6 subsets of informative attributes (IS): $\left\{IS_{SW,i}^{freq}\right\}$, $\left\{IS_{SW,i}^{freq\_cum}\right\}$, $\left\{IS_{MW,i}^{time}\right\}$, $\left\{IS_{MW,i}^{freq}\right\}$, $\left\{IS_{MW,i}^{freq\_cum}\right\}$ with powers:

$$\text{card}\left\{IS_{SW,i}^{time}\right\}=3,\ \text{card}\left\{IS_{SW,i}^{freq}\right\}=2,\ \text{card}\left\{IS_{SW,i}^{freq\_cum}\right\}=2,$$

$$\text{card}\left\{IS_{MW,i}^{time}\right\}=4,\ \text{card}\left\{IS_{MW,i}^{freq}\right\}=2,\ \text{card}\left\{IS_{MW,i}^{freq\_cum}\right\}=2$$

were obtained for each record, respectively.

The complete set of informative attributes:

$$\left\{IS_i\right\}=\left\{IS_{SW,i}^{time}\right\}\cup\left\{IS_{SW,i}^{freq}\right\}\cup\left\{IS_{SW,i}^{freq\_cum}\right\}\cup$$
$$\cup\left\{IS_{MW,i}^{time}\right\}\cup\left\{IS_{MW,i}^{freq}\right\}\cup\left\{IS_{MW,i}^{freq\_cum}\right\},$$

$$\text{card}\left\{IS_i\right\}=15.$$

The formed sets of informative attributes make it possible to conduct a computational experiment to confirm the possibility of barrel classification by the level of wear and assess indicators of the classification quality.

7. A computational experiment with the classification of the barrel wear level

The IS subsets formed in Section 6 were further used in the classification problem. The training and test sets of informative attributes for the classifier were formed on the basis of their estimates normalized to the interval [0, 1] for the records of signals from shots of defect-free and worn barrels corresponding to two classes of the objects being classified. Denote the sets of estimates of informative attributes of defect-free and worn barrels as follows:

$$\mathbf{SB}=\left\{\mathbf{SB}_1,\mathbf{SB}_2,\ldots,\mathbf{SB}_m\right\}, \quad (15)$$

$$\mathbf{WB}=\left\{\mathbf{WB}_1,\mathbf{WB}_2,\ldots,\mathbf{WB}_m\right\}, \quad (16)$$

where

$$SB_i=\left(sb_{i,1},sb_{i,2},\ldots,sb_{i,K}\right)^{\mathrm{T}},$$

$$WB_i=\left(wb_{i,1},wb_{i,2},\ldots,wb_{i,K}\right)^{\mathrm{T}}$$

are the vectors in which each element contains a sequence of normalized informative attributes estimated by the *i*-th record of each set; *K* is the number of records for each type of barrels (*K*=150). Within the corresponding sets, the record numbers *i* were randomly chosen with the exclusion of repetition.

The training data matrix **XC** (that is, rows of the **XC** matrix correspond to the attribute descriptions of the training objects and columns of the matrix correspond to the attributes identified in each record) [51] was defined as

$$\mathbf{XC}=\left\{\mathbf{x}_1^{(s)},\mathbf{x}_2^{(s)},\ldots,\mathbf{x}_m^{(s)},\mathbf{x}_1^{(w)},\mathbf{x}_2^{(w)},\ldots,\mathbf{x}_m^{(w)}\right\}, \quad (17)$$

where

$$\mathbf{x}_i^{(s)}=\left(sb_{i,1},sb_{i,2},\ldots,sb_{i,\delta}\right) \text{ and } \mathbf{x}_i^{(w)}=\left(wb_{i,1},wb_{i,2},\ldots,wb_{i,\delta}\right),$$

$$i=\overline{1,m};$$

δ is the length of the x_i vector taken equal to 100.

The **XT** test matrix was formed in the same way but the vector length x_i was assumed to be 40. The SVM signal classifier was trained and the classification quality was tested using the MATLAB system Statistics and Machine Learning Toolbox. In this case, the MATLAB svmtrain() and svmclassify() functions were used [52]. To assess the information content of the selected attributes, several sets of training and test data were compiled from various IF subsets. The used sets of informative attributes for SVM classification were conventionally called SVM_i, $i=\overline{1,9}$. Since the classification results are binary, the only indicator of the classification quality is the probability of correct classification assessed as

$$\hat{p}_{corr\_class}=N^*/N_{TS}, \quad (18)$$

where N^* is the number of objects correctly assigned to the corresponding classes; N_{TS} is the total amount of the test sampling.

Description of the classification results for various attribute sets is given in Table 1 (the amount of the training sampling is 100, the amount of the test sampling is 40).

The indicators of classification quality are graphically presented in Fig. 11.

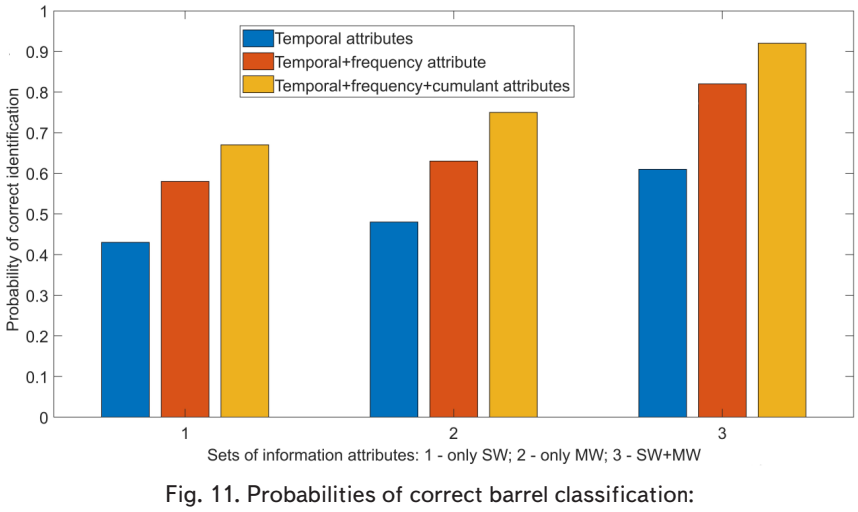

Fig. 11. Probabilities of correct barrel classification:
1 – a set of informative attributes based on the SW analysis only;
2 – a set of informative attributes based on the MW analysis only;
3 – a set of informative attributes based on the SW+MW analysis

Table 1

Description of sets of informative attributes of the SVM classifier

SWM *i*: sets of informative attributes	N / $\hat{p}_{corr\_class}$
SWM1: SW, only temporal attributes $\left\{IS_{BW,i}^{time}\right\}$	52/0.43
SWM2: SW, temporal+frequency attributes $\left\{IS_{BW,i}^{freq}\right\}$	68/0.58
SWM3: SW, temporal+frequency+cumulant attributes $\left\{IS_{BW,i}^{freq\_cum}\right\}$	79/0.67
SWM4: MW, only temporal attributes $\left\{IS_{MW,i}^{time}\right\}$	57/0.48
SWM5: MW, temporal+frequency attributes $\left\{IS_{MW,i}^{freq}\right\}$	76/0.63
SWM6: MW, temporal+frequency+cumulant attributes $\left\{IS_{MW,i}^{freq\_cum}\right\}$	90/0.75
SWM7: SW+MW, only temporal attributes $\left\{IS_{MW,i}^{time}\right\}$	73/0.61
SWM8: SW+MW, temporal+frequency attributes $\left\{IS_{MW,i}^{freq}\right\}$	98/0.82
SWM9: SW+MW, temporal+frequency+cumulant attributes $\left\{IS_{MW,i}^{freq\_cum}\right\}$	110/0.92

Fig. 11 clearly demonstrates the main result of the study: the use of a full set of informative attributes makes it possible to classify defect-free and worn barrels with a probability of correct classification of 0.94.

8. Discussion of results of the assessment of barrel wear using acoustic signals from shots

Let us consider the main results of this study.

A simulation model of acoustic SW and MW signals resulting from artillery shots of barrels with various levels of wear has been developed (expressions (7), (8)). The model is based on the assumption that a shot from a gun with a worn barrel, ceteris paribus (the type of gun, charge, firing conditions) is equivalent to a shot from a gun of reduced caliber. For a simulated real firing situation presented in Fig. 5, a set of 300 synthesized records has been formed. They simulated signals of shots from barrels with various levels of wear. Field records [35], the Wightman model (2), (3) for SW and Berlage model (5) for MW were used in the formation of the synthesized records. In addition, the formation of synthesized records took into account the phenomenon of MW reverberation (12) and additive wind noise (Fig. 7). A typical view of the synthesized record is shown in Fig. 8.

Informative attributes of signals for automatic identification of barrels by the degree of their wear were extracted. Informative attributes for the SW and MW were identified both in the time domain and in the spectral domain (Fig. 9). Cumulant spectral attributes (spectrum kurtosis and spectrum skewness) (13) and (14) based on kurtograms of the shot signals (Fig. 10) were also extracted.

A method of binary classification of artillery barrel by the level of wear was developed based on the extraction of informative attributes (15) to (17) and the SVM classification algorithm.

A computational experiment was carried out to classify the level of barrel wear. Classification quality indicators are shown in Fig. 10. A computational experiment has shown that the selection of attributes for dividing the barrels into two classes was done correctly. The following facts were established in the experiment:

– quality of barrel classification improves when using both SW and MW attributes;

– despite theoretical equivalence of temporal and spectral representation of the signals, the combination of these attributes also makes it possible to improve the quality of barrel classification;

– cumulant spectral attributes (spectrum kurtosis and spectrum skewness) used in the analysis of acoustic signals from shots in combination with conventional indicators can significantly improve the quality of classification.

Thus, all objectives of the study were fulfilled. The possibility of assessing the wear of artillery barrels by the SW and MW signals arising from a shot was demonstrated in the study.

The proposed method of identifying worn barrels has positive qualities in comparison with other known methods of wear assessment:

– a minimal set of auxiliary equipment is required for its implementation in the field: several microphones, a wired communication line, and a computer of a field make;

– the proposed method is prompt. It is assumed that its software has a pre-trained SVM classifier. Then an assessment of belonging of the barrel to one of two classes can be obtained practically in real time. It is only necessary to shoot the number of shots necessary for the formation of a test sample for the assessed gun;

– the method of assessing barrel wear can be used in parallel with the solution of other firing tasks having different objectives but carried out with significant use of shells, for example, during training firing;

– in order to improve the quality of identification, the training sample can be accumulated previously for a long time if guns of the same type are operated at this firing position.

The main limitation of the method proposed as the study result consists in its applicability to only one type of guns with the same barrel model. For other types of guns, it is necessary to form a new training set and train the SVM classifier. However, taking into account the minimum set of equipment necessary for the practical use and availability of numerous software tools for SVM classification, this limitation is easily overcome.

The study results are not yet exhaustive. In particular, the study did not touch upon consideration of meteorology of the bottom layer of atmosphere although it is known that sound velocity in air, frequency-dependent attenuation of acoustic waves, etc. largely depends on meteorological parameters. Assessment of the effect of meteorological parameters on the results of barrel classification using the acoustic fields of shots is the subject of further studies.

9. Conclusions

1. Analysis of models and available experimental data on the SW and MW has shown that they differ significantly. The SW has a characteristic N-shape, duration of 3–5 ms, and a spectrum in the range from 10 to 500–700 Hz. It exists only within the Mach cone formed by a shell flying at supersonic velocity. The MW is a form of a damped oscillatory process lasting 20–50 ms. It is quite accurately described by

the Berlage analytic model. The width of the MW spectrum is 40–60 Hz. Parameters of both SW and MW significantly depend on the initial velocity of the shell. This has made it possible to relate the level of the barrel wear to the parameters of acoustic waves accompanying the shot.

2. Based on the experimental data recorded in the firing of a 155 mm howitzer, a set of 300 synthesized records of acoustic signals simulating shots from barrels with various levels of wear was formed. When forming the data set, actual factors existing during recording the shot sound signals in the bottom layer of the atmosphere were taken into account as much as possible. It was shown that the wind noise with a characteristic spectral density is the main type of interference in this situation. Wind noise was modeled by the "pink noise" model and additively overlaid on the records. The effect of surface reverberation on the MW waveform was also taken into account.

3. Three groups of characteristic attributes were extracted for the classification of barrels by acoustic signals for the SW and MW. The first group includes attributes in the time domain and the second group includes attributes of the spectral domain. For analysis of acoustic signals from shots, cumulant attributes in the spectral domain were used in addition to conventional attributes: a spectrum kurtosis and a spectrum skewness which were attributed to the third group of attributes. Vectors of informational attributes of the SW and MW were formed according to the attributes in all groups.

4. A computational experiment with a binary classification of barrels was performed. The support vector method (SVM classifier) was used as a classifier. It was established in the course of the experiment that the best classification results are achieved by applying the full (temporal and frequency) attribute-based description for the SW and MW. It should be emphasized that the cumulant attributes can significantly improve the classification quality. In terms of correct recognition, the achieved quality of dividing the barrels into defect-free and worn classes was assessed as 0.94.

The study results make it possible to recommend the proposed method for assessing the barrel quality based on the analysis of the acoustic signals accompanying the shot for practical application in the front-line artillery units. The method under study combines minimum requirements for special equipment, efficiency, and high reliability of classification.

References

1. Zakamennyh, I., Kucherova, V. G., Chervontseva, S. E. (Eds.) (2017). Proektirovanie spetsmashin, Ch. 1, Kn. 1. Artilleriyskie stvoly. Volgograd, 396.
2. Pushkarev, A. M. (2018). Elementy teorii iznosa artilleriyskih stvolov. V Vserossiyskaya nauchno-prakticheskaya konferentsiya «Kalashnikovskie chteniya». Izhevsk, 87–92.
3. Li, X., Mu, L., Zang, Y., Qin, Q. (2020). Study on performance degradation and failure analysis of machine gun barrel. Defence Technology, 16 (2), 362–373. doi: https://doi.org/10.1016/j.dt.2019.05.008
4. Banerjee, A., Nayak, N., Giri, D., Bandha, K. (2019). Effect of Gun Barrel Wear on Muzzle Velocity of a typical Artillery Shell. 2019 International Conference on Range Technology (ICORT). doi: https://doi.org/10.1109/icort46471.2019.9069641
5. Maciąg, P., Chałko, L. (2019). Use of sound spectral signals analysis to assess the technical condition of mechanical devices. MATEC Web of Conferences, 290, 01006. doi: https://doi.org/10.1051/matecconf/201929001006
6. Zhitnik, V. E., Petrenko, V. N., Trofimenko, P. E., Gridin, V. I. (2011). Calculation of conditions of the departure of the shell from the trunks canal by means of ballistic station. Systemy ozbroiennia i viyskova tekhnika, 2 (26), 49–52.
7. Pinezich, J. D., Heller, J., Lu, T. (2010). Ballistic Projectile Tracking Using CW Doppler Radar. IEEE Transactions on Aerospace and Electronic Systems, 46 (3), 1302–1311. doi: https://doi.org/10.1109/taes.2010.5545190
8. Ka, M.-H., Vazhenin, N. A., Baskakov, A. I., Oh, C.-G. (2005). Analysis of Power Performance of a Muzzle Velocity Radar. 2005 5th International Conference on Information Communications & Signal Processing. doi: https://doi.org/10.1109/icics.2005.1689038
9. Zubkov, A. N., Kashin, S. V., Leshchenko, S. I., Lob, Ya. D., Martyugov, S. A., Naumets, N. A. et. al. (2009). Artilleriyskaya ballisticheskaya stantsiya novogo pokoleniya. Artilleriyskoe i strelkovoe vooruzhenie, 4, 15–18.
10. Budaretskiy, Y. I. (2015). Ways to increase the firing from cannons with the significant depreciation of the barrel. Systems of Arms and Military Equipment, 2 (42), 7–9.
11. Pushkaryov, A. M., Vershinin, A. A., Volf, I. G. (2015). Estimation of artillery barrel wear. Izvestiya Tul'skogo gosudarstvennogo universiteta. Tehnicheskie nauki, 12 (1), 242–248.
12. Alchinov, V. I., Sidorov, L. I., Chistova, G. K. (2019). Nadezhnost' tehnicheskih sistem voennogo naznacheniya. Moscow: Infra-Inzheneriya, 324.
13. Jain, J., Soni, S., Sharma, D. (2011). Determination of Wear Rate Equation and Estimation of Residual Life of 155mm Autofrettaged Gun Barrel. The International Journal of Multiphysics, 5 (1), 1–8. doi: https://doi.org/10.1260/1750-9548.5.1.1
14. Tsybulyak, B. (2016). Parameters degradation barrel artillery equipment during exploitation. Viyskovo-tekhnichnyi zbirnyk, 14, 121–126.
15. Jankovych, R., Beer, S. (2011). T-72 tank barrel bore wear. International journal of mechanics, 5 (4), 353–360. Available at: http://www.naun.org/main/NAUN/mechanics/17-292.pdf

16. Goncharenko, P. D., Haykov, V. L. (2012). Sovremennye sredstva kontrolya iznosa kanala orudiynogo stvola. Zbirnyk naukovykh prats akademiyi viiskovo-morskykh syl im. P.S. Nakhimova, 1 (9), 22–30.
17. Haykov, V. L. (2013). Development of instrumental control methods and visualization of a gun barrels condition. Eastern-European Journal of Enterprise Technologies, 3 (7 (63)), 52–56. Available at: http://journals.uran.ua/eejet/article/view/14825/12627
18. Zheng, D., Tan, H., Zhou, F. (2017). A design of endoscopic imaging system for hyper long pipeline based on wheeled pipe robot. AIP Conference Proceedings, 1820, 060001. doi: https://doi.org/10.1063/1.4977316
19. Sokolov, A. V., Nasedkin, V. I., Kryuchkov, P. A., Naumov, D. N., Savinyh, S. A., Nikitin, I. S., Devyatkin, V. A. (2014). Optiko-elektronnaya sistema kontrolya iznosa kanalov stvolov. Oboronnaya tehnika, 10, 20–25.
20. Suh, K. (2018). A design on robot system for artillery barrel inspection. International Journal of Pure and Applied Mathematics, 118 (19), 1835–1844. Available at: https://acadpubl.eu/jsi/2018-118-19/articles/19b/21.pdf
21. Slutsky, V. E., Zaycev, A. A. (2014). On procedures of handling the ballistic preparation of artillery systems by applying the equipment of the check & test vehicle. Trudy Nizhegorodskogo gosudarstvennogo tehnicheskogo universiteta im. R.E. Alekseeva, 5 (107), 160–165.
22. Chang, H., Wu, Y.-C., Tsung, T.-T. (2011). Characteristics and measurement of supersonic projectile shock waves by a 32-microphone ring array. Review of Scientific Instruments, 82 (8), 084902. doi: https://doi.org/10.1063/1.3622044
23. Guo, S., Ma, Q., Zhou, X., Shao, R. (2012). Acoustic Recognition of Artillery Projectiles by SVM. Lecture Notes in Electrical Engineering, 345–351. doi: https://doi.org/10.1007/978-3-642-25781-0_52
24. Dagallier, A., Cheinet, S., Cosnefroy, M., Rickert, W., Weßling, T., Wey, P., Juvé, D. (2019). Long-range acoustic localization of artillery shots using distributed synchronous acoustic sensors. The Journal of the Acoustical Society of America, 146 (6), 4860–4872. doi: https://doi.org/10.1121/1.5138927
25. Damarla, T. (2015). Battlefield Acoustics. Springer. doi: https://doi.org/10.1007/978-3-319-16036-8
26. Akman, Ç. (2017). Multi shooter Localization with Acoustic Sensors. Available at: http://etd.lib.metu.edu.tr/upload/12621435/index.pdf
27. Makinen, T., Pertila, P., Auranen, P. (2009). Supersonic bullet state estimation using particle filtering. 2009 IEEE International Conference on Signal and Image Processing Applications. doi: https://doi.org/10.1109/icsipa.2009.5478625
28. Sergienko, A. B. (2011). Tsifrovaya obrabotka signalov. Sankt-Peterburg: BHV-Peterburg, 768.
29. Zhao, X. Y., Zhou, K. D., He, L., Lu, Y., Wang, J., Zheng, Q. (2019). Numerical Simulation and Experiment on Impulse Noise in a Small Caliber Rifle with Muzzle Brake. Shock and Vibration, 2019, 1–12. doi: https://doi.org/10.1155/2019/5938034
30. Maher, R. C., Shaw, S. R. (2008). Deciphering gunshot recordings. 33rd International Conference: Audio Forensics-Theory and Practice. Available at: http://www.aes.org/e-lib/browse.cfm?elib=14410
31. Naz, P., Marty, C. (2006). Sound detection and localization of small arms, mortars, and artillery guns. Unattended Ground, Sea, and Air Sensor Technologies and Applications VIII. doi: https://doi.org/10.1117/12.672936
32. Rabinovich, E. V., Filipenko, N. Y., Shefel, G. S. (2018). Generalized model of seismic pulse. Journal of Physics: Conference Series, 1015, 052025. doi: https://doi.org/10.1088/1742-6596/1015/5/052025
33. ISO 9613-1:1993. Acoustics – Attenuation of sound during propagation outdoors – Part 1: Calculation of the absorption of sound by the atmosphere (1993). ISO, 26.
34. Bykov, A. P., Medvetskiy, S. V. (2010). K voprosu o koeffitsientah, harakterizuyushchih vnutriballisticheskiy protsess klassicheskogo artilleriyskogo vystrela. Izvestiya Rossiyskoy akademii raketnyh i artilleriyskih nauk, 2 (64), 75–80.
35. Huseby, M. (2007). Noise emission data for M109, 155 mm field howitzer. Norwegian Defence Research Establishment (FFI), 45. Available at: https://publications.ffi.no/nb/item/asset/dspace:3388/07-02530.pdf
36. Field Artillery Sound Ranging and Flash Ranging (1979). United States. Department of the Army, Headquarters, 231. Available at: https://books.google.com.ua/books/about/Field_Artillery_Sound_Ranging_and_Flash.html?id=0IhyEWUhBCsC&redir_esc=y
37. Loucks, R. B., Davis, B. S., Moss, L. G., Pham, T., Fong, M. (1995). A Method of Identifying Supersonic Projectiles Using Acoustic Signatures. USA ARL, 223. Available at: https://apps.dtic.mil/dtic/tr/fulltext/u2/a299215.pdf
38. Belov, V. V., Burkatovskaya, Yu. B., Krasnenko, N. P., Rakov, A. S., Rakov, D. S., Shamanaeva, L. G. (2018). Experimental and theoretical investigations of near-ground acoustic radiation propagation in the atmosphere. Atmospheric and Oceanic Optics, 5, 372–377. doi: https://doi.org/10.15372/aoo20180506
39. Hacıhabiboğlu, H. (2017). Procedural Synthesis of Gunshot Sounds Based on Physically Motivated Models. Game Dynamics, 47–69. doi: https://doi.org/10.1007/978-3-319-53088-8_4
40. Wilson, D. K., White, M. J. (2010). Discrimination of Wind Noise and Sound Waves by Their Contrasting Spatial and Temporal Properties. Acta Acustica United with Acustica, 96 (6), 991–1002. doi: https://doi.org/10.3813/aaa.918362
41. Becker, G., Güdesen, A. (2000). Passive sensing with acoustics on the battlefield. Applied Acoustics, 59 (2), 149–178. doi: https://doi.org/10.1016/s0003-682x(99)00023-7

42. Dutoit, T., Marqués, F. (2009). Applied Signal Processing. A MATLAB™-Based Proof of Concept. Springer. doi: https://doi.org/10.1007/978-0-387-74535-0
43. Kirsanov, E. A., Sirota, A. A. (2012). Obrabotka informatsii v prostranstvenno-raspredelennyh sistemah radiomonitoringa: statisticheskiy i neyrosetevoy podhody. Moscow: Fizmatlit, 344.
44. Al-Jasri, G. Kh. M., Boltenkov, V. A., Chervonenko, P. P. (2016). Algoritms of cooperative heat trasfer leak detection in acoustic sensor nework. Elektrotekhnichni ta kompiuterni systemy, 21 (97), 92–97.
45. Awad, M., Khanna, R. (2015). Support Vector Machines for Classification. Efficient Learning Machines, 39–66. doi: https://doi.org/10.1007/978-1-4302-5990-9_3
46. Wang, L. (2005). Support Vector Machines: Theory and Applications. Springer. doi: https://doi.org/10.1007/b95439
47. Temko, A., Nadeu, C. (2006). Classification of acoustic events using SVM-based clustering schemes. Pattern Recognition, 39 (4), 682–694. doi: https://doi.org/10.1016/j.patcog.2005.11.005
48. Hägele, D., Schefczik, F. (2018). Higher-order moments, cumulants, and spectra of continuous quantum noise measurements. Physical Review B, 98 (20). doi: https://doi.org/10.1103/physrevb.98.205143
49. Antoni, J., Randall, R. B. (2006). The spectral kurtosis: application to the vibratory surveillance and diagnostics of rotating machines. Mechanical Systems and Signal Processing, 20 (2), 308–331. doi: https://doi.org/10.1016/j.ymssp.2004.09.002
50. Hixon, T. J., Weismer, G., Hoit, J. D. (2014). Preclinical speech science: Anatomy, physiology, acoustics, perception. Plural Publishing. Available at: https://psycnet.apa.org/record/2013-10861-000
51. Demidova, L. A., Sokolova, Y. S. (2017). Two-stage data classification method based on SVM-algorithm and the k nearest neighbors algorithm. Vestnik of Ryazan State Radio Engineering University, 62, 119–132. doi: https://doi.org/10.21667/1995-4565-2017-62-4-119-132
52. Algazinov, E. K., Dryuchenko, M. A., Minakov, D. A., Sirota, A. A., Shulgin, V. A. (2013). Methods pattern recognition elements of cereal mixes of results spectral characteristics in the separation system real time. Vestnik Voronezhskogo gosudarstvennogo universiteta. Seriya: Sistemniy analiz i informatsionnye tehnologii, 2, 9–19.